MATHEMATICAL BIOSCIENCES
AND ENGINEERING
Volume **11**, Number **1**, February **2014**

doi:10.3934/mbe.2014.11.49

pp. **49–62**

ESTIMATING NONSTATIONARY INPUTS FROM A SINGLE SPIKE TRAIN BASED ON A NEURON MODEL WITH ADAPTATION

Hideaki Kim

NTT Service Evolution Laboratories, NTT Corporation
Yokosuka-shi, Kanagawa, 239-0847, Japan

Shigeru Shinomoto

Department of Physics, Graduate School of Science, Kyoto University
Sakyo-ku, Kyoto 606-8502, Japan

Abstract. Because every spike of a neuron is determined by input signals, a train of spikes may contain information about the dynamics of unobserved neurons. A state-space method based on the leaky integrate-and-fire model, describing neuronal transformation from input signals to a spike train has been proposed for tracking input parameters represented by their mean and fluctuation [11]. In the present paper, we propose to make the estimation more realistic by adopting an LIF model augmented with an adaptive moving threshold. Moreover, because the direct state-space method is computationally infeasible for a data set comprising thousands of spikes, we further develop a practical method for transforming instantaneous firing characteristics back to input parameters. The instantaneous firing characteristics, represented by the firing rate and non-Poisson irregularity, can be estimated using a computationally feasible algorithm. We applied our proposed methods to synthetic data to clarify that they perform well.

1. **Introduction.** Neuroscience researchers have measured neuronal firing rates in correlation to animals' behavior, largely ignoring the detailed patterns of spike times. In this paper, we examine spike timing to collect additional information about the dynamics of unobserved neuronal populations, on the basis of the assumption that neuronal spike timing can provide information about the population activities of excitatory and inhibitory neurons.

Each cortical neuron constantly receives spiking signals from thousands of other neurons. The random arrival of a number of synaptic inputs results in uncorrelated fluctuations that can be characterized by their mean and amplitude, and these can be related to the activities of presynaptic excitatory and inhibitory neuronal populations. Mathematical methods have been developed to infer the input parameters from firing characteristics on the basis of the assumption that presynaptic neuronal activities are constant across time [8, 5, 13, 20].

However, the stationary input conditions assumed by the standard leaky integrate-and-fire (LIF) model [34] cannot account for the spiking statistics of cortical neurons in vivo [32, 28, 26]. Some studies have suggested resolving this inconsistency

2010 *Mathematics Subject Classification.* Primary: 60H30, 62P10; Secondary: 65C30.

Key words and phrases. Input estimation, neuronal model, spike data, spike frequency adaptation, Bayesian analysis, state-space method, method of moments, first-passage time.

by introducing nonstationary or correlated fluctuations to the inputs [32, 26]. Recently, to track temporal variation of input parameters representing the mean and the amplitude of uncorrelated fluctuations, several methods have been proposed using time-dependent stimulus traces [22] or averaging over repeated trials [37]. More recently, a method for estimating input parameters in a single trial has been suggested, based on the LIF model with current synapses [11].

However, the LIF model does not exhibit the adaptation that has been observed in a majority of pyramidal cells *in vitro* [19, 17] and this is believed to cause the correlations between successive interspike intervals (ISIs) that have been observed in spike trains recorded *in vivo* [16, 21, 6, 1]. In this paper, we propose improving the input estimation method by incorporating an adaptive threshold into the LIF model. We examine the direct state-space method for carrying out the Bayesian inference of input parameters, and show that it has an enormous computational complexity that makes it infeasible for a train of a thousand spikes. In addition, to make input estimation feasible for massive data, we propose a method for transforming neuronal firing characteristics into input parameters. The firing characteristics consisting of the instantaneous firing rate and firing irregularity are estimated using a computationally feasible state-space method that can efficiently process larger amounts of data [27]. To make it possible to track inputs with parameters representing their mean and fluctuation, we construct a computationally feasible transformation method. We test our proposed methods using synthetic data generated by the numerical simulations of the generative model.

2. Generative models.

To infer the firing activities of excitatory and inhibitory neuronal populations from a train of evoked spikes, we need a forward generative model that transforms the input signal into an output spike train. Recently, it has been proposed that input parameters can be estimated using a basic LIF model [11]. In this paper, we propose an efficient method of estimating inputs and apply this method not only to the basic LIF model but also to an adaptive threshold LIF model, which represents a more realistic neuronal transformation.

2.1. The leaky integrate-and-fire (LIF) model.

The LIF model is a succinct model representing basic neuronal firing mechanisms, given by

$$\begin{aligned} \tau_{\mathrm{m}} \frac{dV(t)}{dt} &= V_{\mathrm{l}} - V(t) + RI(t), \\ \text{if } V(t) > V_{\mathrm{th}}&, \text{ then } V(t) \to V_{\mathrm{reset}}, \end{aligned} \tag{1}$$

where τ_{m}, V_{l}, V_{th}, V_{reset}, R, and $I(t)$ represent the membrane time constant, resting potential, threshold potential, resetting potential, membrane resistance, and input current, respectively. We set these parameters to values that have been adopted in the literature [19, 18, 33]: $\tau_{\mathrm{m}} = 20$ ms, $V_{\mathrm{l}} = $ -75 mV, $V_{\mathrm{th}} = $ -55 mV, $V_{\mathrm{reset}} = V_{\mathrm{th}} - 6 = $ -61 mV, and $R = 40$ MΩ.

To represent inputs, we adopted Stein's model [34], in which the membrane potential is increased or decreased by a fixed amount, called the excitatory and the inhibitory post-synaptic potential (EPSP and IPSP), respectively, on the arrival of each input spike signal. Thus, every input current is represented by a delta function of time with a fixed positive or negative coefficient.

It is well known that each cortical neuron constantly receives signals from thousands of neurons. If EPSPs and IPSPs occur at randomly in time and have small

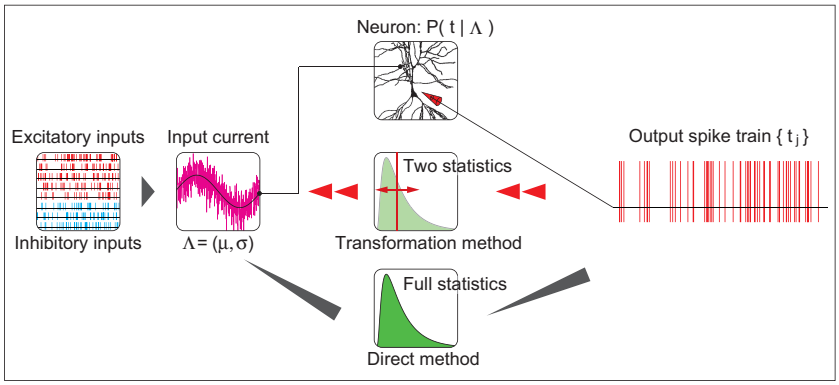

FIGURE 1. A schema for the estimation procedure. A neuron constantly receives excitatory and inhibitory synaptic inputs, of which sum can be approximated as a current with a mean μ and a fluctuation $\sigma\xi(t)$. We estimate the input parameters (μ, σ) from a single output spike train $\{t_j\}$, based on the direct and transformation methods. In the direct method, we compute the full statistics of the data, that is, the probability of the spike train occurring, and find the most probable input parameters. In the transformation method, we estimate the two firing characteristics of the spike data, that is, the rate (mean of ISI) and irregularity (variance of ISI), and transform their information into likely input parameters.

amplitudes, the input current can be approximated as a diffusion process with a mean drift μ and temporally uncorrelated (white) fluctuation $\sigma\xi(t)$ [12],

$$I(t) = \mu + \sigma\xi(t), \tag{2}$$

where $\xi(t)$ is white noise satisfying the ensemble statistics $\langle\xi(t)\rangle = 0$ and $\langle\xi(t)\xi(t')\rangle = \delta(t - t')$. Assuming white Gaussian inputs, the interspike interval (ISI) is given by the first-passage time distribution of the Ornstein-Uhlenbeck process (OUP) [34].

2.2. **The adaptive LIF model.** No renewal process, including the basic LIF models described above, is capable of reproducing the spike-frequency adaptation observed in a majority of pyramidal cells [19, 17], which is believed to cause the correlation between successive ISIs observed in recorded spike trains [16, 21, 6, 1].

However, it is known that the spike-frequency adaptation can be realized by modifying the LIF model in such a way that the threshold is dynamically modulated as follows:

$$\theta(t) = V_{\text{th}} + \Delta_S \sum_j \exp[-(t - t_j)/\tau_{\text{ad}}], \tag{3}$$

where V_{th} is the baseline threshold value, t_j is the jth output spike time, τ_{ad} is the adaptation time constant, and Δ_S is an increment that is added to the threshold potential at each spike to suppress the firing activity. We set the model parameters at values that have been adopted in the literature [16, 2]: $V_{\text{reset}} = V_{\text{th}} - 10 = -65$ mV, $\tau_{\text{ad}} = 100$ ms, and $\Delta_S = 2$ mV, with other parameters remaining the same as those in the basic LIF model.

3. Estimating input parameters (I): The direct state-space method.

3.1. The state-space method for an LIF model.

Input parameters representing the mean and fluctuation of the input current $\Lambda = (\mu, \sigma^{-1})$ can be inferred from the spike times $\{t_j\}_{j=0}^n = \{t_0, t_1, t_2, \cdots, t_n\}$ by using Bayes' rule for the forward spiking neuron model given in the above Eq. (1):

$$P(\Lambda(t)|\{t_j\}) = \frac{P(\{t_j\}|\Lambda(t))P(\Lambda(t))}{P(\{t_j\})}. \tag{4}$$

When the generative model is based on a renewal process, the probability of a spike train occurring is factorized into probabilities of having ISIs:

$$P(\{t_j\}|\Lambda) = \prod_{j=1}^{n} P(s_j|\Lambda), \tag{5}$$

where $s_j \equiv t_j - t_{j-1}$ is the jth ISI. For time-varying input parameters $\Lambda(t)$, given the momentary input conditions, $\Lambda_{j-1} \equiv \Lambda(t_{j-1})$, we approximate the probability as the product of probabilities of ISIs:

$$P(\{t_j\}|\Lambda(t)) = \prod_{j=1}^{n} P(s_j|\Lambda_{j-1}). \tag{6}$$

Note that the constancy of the input parameters during each ISI does not mean that the input current was constant; rather, the input current has fluctuated in an amplitude σ, reflecting a number of input spikes coming from the presynaptic populations of excitatory and inhibitory neurons.

To model the prior distribution of the input parameters represented by the two-dimensional vector $\Lambda(t) \equiv (\Lambda^1(t), \Lambda^2(t))$, we incorporate the tendency to vary slowly by penalizing large gradients:

$$P(\Lambda(t)) = \prod_{j=1}^{n} P_\gamma(\Lambda_j|\Lambda_{j-1}) \propto \prod_{j=1}^{n}\prod_{k=1}^{2} \exp\left(-\frac{(\Lambda_j^k - \Lambda_{j-1}^k)^2}{2\gamma^k s_j}\right), \tag{7}$$

where $\gamma \equiv (\gamma^1, \gamma^2)$ is a hyperparameter representing the stationarity of the input parameters. This is equivalent to the assumption that input parameters be exhibiting a random walk; therefore, the variance should be rescaled with the ISI, $s_j = t_j - t_{j-1}$. The initial parameter $\Lambda_0 \equiv ({\Lambda^1}_0, {\Lambda^2}_0)$ was set to the value that have been estimated on the basis of the assumption that input parameters are constant over time.

The hyperparameters $\gamma \equiv (\gamma^1, \gamma^2)$ can be determined by a principle of the empirical Bayes method, namely by maximizing the marginal likelihood, $P_\gamma(\{t_j\}) = \prod_{j=1}^n \int d\Lambda_{j-1} P(s_j|\Lambda_{j-1}) P_\gamma(\Lambda_j|\Lambda_{j-1})$. Given a specific set of spike times, the marginal likelihood function can be maximized using the Expectation Maximization (EM) algorithm [29]. In the EM algorithm, hyperparameters are determined by iteratively maximizing the expected value of the log-likelihood function, Q:

$$\begin{aligned} Q(\gamma|\gamma_{(p)}) &= \mathrm{E}[\log P_\gamma(\{t_j\}, \{\Lambda_j\})|\{t_j\}, \gamma_{(p)}] \\ &= \sum_{j=1}^{n} \mathrm{E}[\log P_\gamma(\Lambda_j|\Lambda_{j-1})|\{t_j\}, \gamma_{(p)}] \\ &+ \sum_{j=1}^{n} \mathrm{E}[\log P(s_j|\Lambda_{j-1})|\{t_j\}, \gamma_{(p)}], \end{aligned} \tag{8}$$

where $\gamma_{(p)} \equiv (\gamma^1_{(p)}, \gamma^2_{(p)})$ is the set of hyperparameters for the pth iteration, and $\mathrm{E}[\dot{|}\{t_j\}, \gamma_{(p)}]$ represents the expectation with respect to the conditional distribution of Λ given $\{t_j\}_{j=0}^n$ under the pth estimate of the hyperparameters. The $(p+1)$st estimate of γ is determined by the conditions for $dQ/d\gamma = 0$, leading to the following equation:

$$\gamma^k_{(p+1)} = \frac{1}{n-1} \sum_{j=1}^{n-1} \frac{1}{s_j} \mathrm{E}\Big[(\Lambda^k_{j+1} - \Lambda^k_j)^2 | \{t_j\}, \gamma_{(p)}\Big], \text{ for } k = 1 \text{ and } 2. \tag{9}$$

The expected value appearing on the right hand side of Eq. (9) can be obtained using the Kalman filtering and smoothing algorithm on the basis of the approximation that the filtering distribution of input parameter Λ is Gaussian distributed (Laplace approximation) [29, 27].

3.2. **The state-space method for an adaptive LIF model.** For an adaptive LIF model in which the threshold is moving adaptively, the probability of a spike train occurring can no longer be factorized into the probabilities of ISIs, because the ISI distribution $P(s_j = t_j - t_{j-1} | \Lambda_{j-1})$ is dependent on past firings. However, it is possible to recover the Markov property by including the dynamical threshold or $\Theta_j \equiv \theta(t_j) - V_{\mathrm{th}}$ into dynamical conditions, because the threshold obeys a simple first order recurrence equation:

$$\Theta_j = \Theta_{j-1} \cdot \exp[-s_j/\tau_{\mathrm{ad}}] + \Delta_S. \tag{10}$$

Thus the probability of a spike train occurring is calculated by modifying Eq. (6) to

$$P(\{t_j\} | \Lambda(t)) = \prod_{j=1}^{n} P(s_j | \Lambda_{j-1}, \Theta_{j-1}). \tag{11}$$

The ISI distribution function for the given input conditions can be obtained by solving a second-kind Volterra integral equation [3]. When computing the probability of a spike train occurring (Eqs. (6) and (11)), we used the method proposed by Paninski *et al.* to compute the integral equation efficiently [23]. To perform the numerical integration, we evenly divided the integration interval into 150 small segments.

4. **Estimating input parameters (II): The transformation method.** The direct state-space method introduced above requires heavy computation, particularly in computing the ISI distribution for a set of input parameters, and therefore, even with a high-speed large-capacity computer, we had to limit the analysis to trains of not more than several hundred spikes. It has been suggested that the capacity for input estimation can be increased by introducing a two-step analysis method [11] in which (1) the firing characteristics are estimated using a computationally feasible state-space algorithm, and (2) the firing characteristics are converted into likely input parameters across time by inverting the neuronal forward transformation. In step (1), the instantaneous firing characteristics comprising the firing rate and non-Poisson irregularity can be estimated using a computationally feasible state-space model that can process extremely large data sets containing as many as 1,00,000 spikes [27]. To characterize the ISI distribution, we adopted an exponential family of distribution functions $f_{\lambda,\kappa}(s)$, that are parameterized with a scale factor λ and

a shape factor κ, representing the mean firing rate and the firing irregularity, respectively. A shape factor deviating from $\kappa = 1$ represents non-Poisson irregularity. We can use the state-space method to obtain the maximum *a posteriori* (MAP) estimates of the time-varying firing rate $\hat{\lambda}(t)$ and firing irregularity $\hat{\kappa}(t)$.

In step (2), these firing characteristics are converted into the most likely input parameters, as represented by their means $\hat{\mu}$ and variations $\hat{\sigma}^2$. This is done by using transformation formulas, $\mu = M(\lambda, \kappa)$ and $\sigma = S(\lambda, \kappa)$, that are obtained by inverting the neuronal forward transformation of the input signals to output spiking with $\lambda = L(\mu, \sigma)$ and $\kappa = K(\mu, \sigma)$. It has been suggested that a table or a spline fitting formula be constructed for this purpose, by fitting the gamma distribution to the ISI distribution of the spiking neuron model through the minimization of the Kullback–Leibler (KL) divergence [11].

Here, we consider applying the transformation method to not only the LIF model but also the adaptive LIF model. However, it is difficult to use the proposed technique of using a lookup table for adaptive LIF models that require fitting three parameters. Thus, we suggest another principle which is to fit a two-parameter exponential family of distribution functions $f_{\lambda,\kappa}(s)$ to the empirical ISI distribution of a spiking neuron model $P(s|\mu, \sigma)$ by fitting their low-order moments. That is, the firing characteristics (λ, κ) are converted into the input parameters (μ, σ) on the condition that the means and variances of the ISIs are equal:

$$\mathrm{E}_P[s](\mu, \sigma) = \mathrm{E}_f[s](\lambda, \kappa), \tag{12}$$

$$\mathrm{Var}_P[s](\mu, \sigma) = \mathrm{Var}_f[s](\lambda, \kappa). \tag{13}$$

Here $\mathrm{E}_P[s]$ and $\mathrm{Var}_P[s]$ represent the mean and variance of the ISI distribution $P(s|\mu, \sigma)$, respectively, and $\mathrm{E}_f[s]$ and $\mathrm{Var}_f[s]$ represent those of the exponential family distribution $f_{\lambda,\kappa}(s)$. In the next section, we summarize the methods to obtain the means $\mathrm{E}_P[s]$ and variances $\mathrm{Var}_P[s]$ of ISI distributions, and transform the firing characteristics (λ, κ) into the input parameters (μ, σ), with respect to the non-adaptive and adaptive LIF models, respectively.

Here for the purpose of describing our methods succinctly, we consider a standard Ornstein-Uhlenbeck process model with two independent parameters for the non-adaptive LIF model:

$$\begin{aligned} &\frac{dV(t)}{dt} = -V(t) + \mu + \sigma\xi(t), \\ &\text{if } V(t) > 1, \text{ then } V(t) \to 0. \end{aligned} \tag{14}$$

Also for the adaptive LIF model, we adopt a standard adaptive LIF model:

$$\begin{aligned} \theta(t) &= 1 + \epsilon_{j-1} \exp[-\beta(t - t_{j-1})], \quad t_{j-1} < t < t_j \\ \epsilon_j &= \epsilon_{j-1} \cdot \exp[-\beta s_j] + \Delta_\epsilon, \end{aligned} \tag{15}$$

where $s_j = t_j - t_{j-1}$ is the jth ISI. The ISI distribution of a particular LIF model (see Eqs. (1) and (3) in the main text) can be reconstructed from that of the standard model (Eqs. (14) and (15)) by replacing the variables and parameters in Eqs. (14)

and (15) as:

$$\begin{aligned} t &\to t/\tau_{\mathrm{m}}, \\ \mu &\to R\mu/(V_{\mathrm{th}} - V_{\mathrm{reset}}) + (V_{\mathrm{l}} - V_{\mathrm{reset}})/(V_{\mathrm{th}} - V_{\mathrm{reset}}), \\ \sigma &\to R\sigma/(\sqrt{\tau_{\mathrm{m}}}(V_{\mathrm{th}} - V_{\mathrm{reset}})), \\ \beta &\to \tau_{\mathrm{m}}/\tau_{\mathrm{ad}}, \\ \Delta_\epsilon &\to \Delta_S/(V_{\mathrm{th}} - V_{\mathrm{reset}}). \end{aligned} \tag{16}$$

4.1. **The transformation method for an LIF model.** For standard LIF models (14), the mean and variance of the ISI distribution, denoted by $\mathrm{E}_P^0[s]$ and $\mathrm{Var}_P^0[s]$ respectively, can be calculated quickly with the following equations [10, 25, 28]:

$$\mathrm{E}_P^0[s](\mu,\sigma) = \phi_1(\sqrt{2}\eta_+) - \phi_1(\sqrt{2}\eta_-), \tag{17}$$

$$\mathrm{Var}_P^0[s](\mu,\sigma) = \phi_1^2(\sqrt{2}\eta_+) - \phi_2(\sqrt{2}\eta_+) + \phi_2(\sqrt{2}\eta_-) - \phi_1^2(\sqrt{2}\eta_-), \tag{18}$$

where

$$\begin{aligned} &\eta_+ = (1-\mu)/\sigma, \quad \eta_- = -\mu/\sigma, \\ &\phi_{l=1,2} = \frac{l}{2^l}\sum_{k=1}^{100}\frac{(\sqrt{2}z)^k}{k!}\Gamma\Big(\frac{k}{2}\Big)\rho_k^{(l)}, && : z > -5.70 \\ &\phi_1(z) = -\left(K_B + \log|z| + \sum_{k=1}^{10}\frac{b_k}{z^{2k}}\right), && : z \le -5.70 \\ &\phi_2(z) = 2\left[K_D + K_B\log|z| + \frac{1}{2}(\log|z|)^2\right. \\ &\qquad\qquad \left. + \sum_{k=1}^{10} b_k\frac{\log|z|}{z^{2k}} + \sum_{k=1}^{10}\frac{g_k}{z^{2k}}\right], && : z \le -5.70 \\ &\rho_k^{(1)} = 1, \quad \rho_k^{(2)} = \psi(k/2) - \psi(1), \\ &K_B = 0.63518142, \quad K_D = 0.818578, \\ &a_k = \frac{(-1)^{k-1}(2k-2)!}{(k-1)!2^{k-1}}, \quad b_k = -\frac{a_{k+1}}{2k}, \quad c_k = a_k + b_k, \\ &d_k = c_k - (2k-1)d_{k-1}, \quad g_k = K_B\ b_k - \frac{a_{k+1}}{4k^2} - \frac{d_k}{2k}. \end{aligned} \tag{19}$$

Here $\psi(\cdot)$ denotes the digamma function. Because the derivatives of the mean and variance with respect to the input parameters can also be determined by the set of equations (19), we can solve the moment-matching equations (12) and (13) by the standard Newton-Raphson method [24], given the mean and variance of the ISIs of the exponential family distribution under the specified scale and shape factors, λ and κ.

When executing the Newton-Raphson method, it is essential to choose an appropriate initial value, and this can be obtained as follows. Assuming that $\mu = 1$, the mean, $\mathrm{E}_P^0[s] = -\phi_1(-\sqrt{2/\sigma^2})$, is a monotonically decreasing function of σ, and therefore, the root σ_0 of Eq. (12) can be obtained with the bisection method [24]. Then, beginning with $(1, \sigma_0)$, the root (μ, σ) of Eq. (13) can be sought along the

curve of $\mathrm{E}_P^0[s] = \text{const.}$ [35] satisfying

$$\frac{d\mu}{d\sigma^2} = (\eta_+ - \eta_-)\left[\frac{\eta_+ \exp(\eta_+^2)\mathrm{erf}(-\eta_+) - \eta_- \exp(\eta_-^2)\mathrm{erf}(-\eta_-)}{\exp(\eta_-^2)\mathrm{erf}(-\eta_-) - \exp(\eta_+^2)\mathrm{erf}(-\eta_+)}\right], \tag{20}$$

where $\mathrm{erfc}(z)$ denotes the complementary error function.

4.2. **The transformation method for an adaptive LIF model.** To estimate the ISI distribution for the standard adaptive LIF models (15), we have to take into account the initial value of the moving threshold, $1+\epsilon_j$, at each spike time, in addition to the input parameters. In cases where ϵ_j is small, the mean and variance of the ISI distribution for the adaptive LIF model, denoted by $\mathrm{E}_P^{\epsilon_j}[s]$ and $\mathrm{Var}_P^{\epsilon_j}[s]$ respectively, can be calculated by expanding the mean and variance for the standard LIF model (14) in terms of $\epsilon_j/(1+\epsilon_j)$ [15]:

$$\begin{aligned}\mathrm{E}_P^{\epsilon_j}[s](\mu,\sigma) \simeq\ & \mathrm{E}_P^0[s](\mu',\sigma') \\ & + \frac{\epsilon_j}{1+\epsilon_j}\left\{\frac{\sqrt{\pi}}{\sigma'}\left[\rho_0(\beta)e^{\eta_+'^2}\mathrm{erfc}(-\eta_+') - e^{\eta_-'^2}\mathrm{erfc}(-\eta_-')\right]\right. \\ & \left. + (1-c_1)\frac{\partial}{\partial\mu'}\mathrm{E}_P^0[s](\mu',\sigma')\right\},\end{aligned} \tag{21}$$

$$\begin{aligned}\mathrm{Var}_P^{\epsilon_j}[s](\mu,\sigma) \simeq\ & \mathrm{Var}_P^0[s](\mu',\sigma') \\ & + \frac{\epsilon_j}{1+\epsilon_j}\left\{-\frac{2\sqrt{\pi}}{\sigma'}\left[e^{\eta_+'^2}\mathrm{erfc}(-\eta_+')\left(\frac{d\rho_0}{d\beta} + \rho_0(\beta)\mathrm{E}_P^0[s](\mu',\sigma')\right)\right.\right. \\ & \left.\left. + \sqrt{\pi}J(\eta_-') - \sqrt{\pi}\rho_0(\beta)J(\eta_+')\right] + (1-c_2)\frac{\partial}{\partial\mu'}\mathrm{Var}_P^0[s](\mu',\sigma')\right\},\end{aligned} \tag{22}$$

where

$$\begin{aligned}&\mu' = (\mu + c_1\epsilon_j)/(1+\epsilon_j), && \sigma' = \sigma(1+c_2\epsilon_j)/(1+\epsilon_j), \\ &\eta_+' = (1-\mu')/\sigma', && \eta_-' = -\mu'/\sigma', \\ &J(z) = \frac{d}{dz}\left[\phi_1^2(z) - \phi_2(z)\right], && \rho_0(\beta) = \frac{H_{-\beta}(-\eta_-')}{H_{-\beta}(-\eta_+')}.\end{aligned} \tag{23}$$

Here $H_\nu(z)$ denotes the Hermite function, and can be calculated quickly, when the parameter $|\nu| << 1$, based on the following series expansion formula [14]:

$$H_\nu(z) = \begin{cases} \dfrac{1}{2\Gamma(-\nu)}\displaystyle\sum_{k=0}^{100}\frac{(-1)^k\Gamma(\frac{k-\nu}{2})}{k!}(2z)^k, & |z| < 5.0 \\ \displaystyle\sum_{k=0}^{10}\frac{(-1)^k}{k!}\frac{\Gamma(-\nu+2k)}{\Gamma(-\nu)}(2z)^{\nu-2k} & \\ \quad -\mathbf{I}(-z)\dfrac{\sqrt{\pi}e^{\nu\pi i}}{\Gamma(-\nu)}e^{z^2}z^{-\nu-1}\displaystyle\sum_{k=0}^{10}\frac{\Gamma(\nu+2k+1)}{k!\,\Gamma(\nu+1)}(2z)^{-2k}, & |z| \geq 5.0 \end{cases} \tag{24}$$

where $\mathbf{I}(z)$ is the step function satisfying $\mathbf{I} = 0$ for $z < 0$ and $\mathbf{I} = 1$ for $z > 0$. For this study, we set the two parameters c_1 and c_2, which in general, depend on β, μ and σ, to β^2. Using the roots of Eqs. (12) and (13) for $\epsilon_j = 0$ as a initial point, we can solve the set of equations (12) and (13) for $\epsilon_j \neq 0$ using the standard Newton-Raphson method.

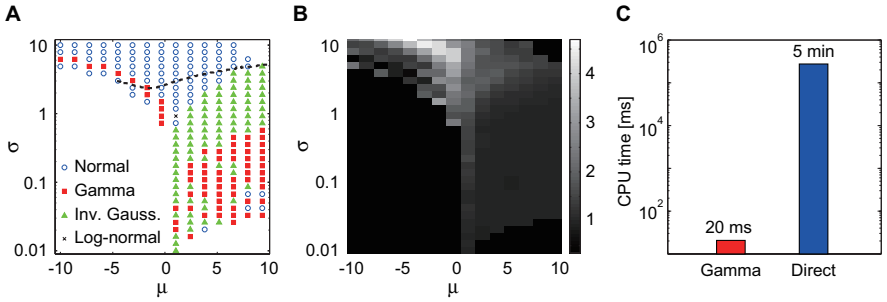

FIGURE 2. Comparison of the direct and transformation methods for estimating stationary input parameters. (A) The parameter ranges with the least average squared errors for the transformation method with the normal, gamma, inverse Gaussian, and log-normal distributions are depicted by *circles*, *squares*, *triangles*, and *cross marks*, respectively. The input region that generates biologically implausible outputs (those in which the firing rate is less than 0.01 or greater than 100 $[1/\tau_m]$, or the Cv is less than 0.01) was not searched. The dashed line represents the contour line of Cv = 1.5. (B) The ratio of the average squared error for the gamma distribution to that for the direct method. (C) Computational costs of the transformation method with the gamma distribution and the direct method for a spike train comprising 1,000 ISIs.

5. **Results.**

5.1. **Comparison of the exponential families of the distribution functions.**

For the application of our method to neurophysiological data, we selected an exponential family of distribution functions based on the accuracy of the input estimation. For this purpose, we compared the normal, gamma, inverse Gaussian, and log-normal distribution functions with respect to their fit to the ISIs generated by the OUP. Here without loss of generality, we set τ_m, R, and $V_{\rm th}$ in Eq. (1) to unit, and $V_{\rm reset}$ and $V_{\rm l}$ to zero (see Eqs. (14)-(16)).

Distribution	$f_{\lambda,\kappa}(s)$	$\mathrm{E}_f[s]$	$\mathrm{Var}_f[s]$
Normal	$\sqrt{\frac{\kappa\lambda^2}{2\pi}}\exp\left[-\frac{\kappa}{2}(1-\lambda s)^2\right]$	$\frac{1}{\lambda}$	$\frac{1}{(\kappa\lambda^2)}$
Gamma	$\kappa\lambda(\kappa\lambda s)^{\kappa-1}\exp\left[-\kappa\lambda s\right]/\Gamma(\kappa)$	$\frac{1}{\lambda}$	$\frac{1}{(\kappa\lambda^2)}$
Inv. Gauss.	$\sqrt{\frac{\kappa}{2\pi s^3}}\exp\left[-\frac{\kappa}{2s\lambda}(1-\lambda s)^2\right]$	$\frac{1}{\lambda}$	$\frac{1}{(\kappa\lambda^2)}$
Log-normal	$\sqrt{\frac{\kappa}{2\pi s^2}}\exp\left[-\frac{\kappa}{2}(\log(s\lambda)+\frac{1}{2\kappa})^2\right]$	$\frac{1}{\lambda}$	$\frac{(e^{1/\kappa}-1)}{\lambda^2}$

TABLE 1. $\Gamma(\kappa)$ denotes the gamma function, and $\mathrm{E}_f[s]$ and $\mathrm{Var}_f[s]$ are the mean and variance of each distribution $f_{\lambda,\kappa}(s)$, respectively. The parameters in the exponential families represent the firing characteristics of the spike data: λ represents the firing rate, and κ represents irregularity.

Given a set of input parameters (μ, σ) and dividing the spike train into m short spike trains each comprising 100 ISIs, we generated $100 \times m$ ISIs with the OUP and repeatedly estimated the input parameters from each spike train. To investigate the suitability of the distributions for the moment-matching strategy (Eqs. (12) and (13)), we assumed that the input parameters to be estimated are constant, that is, we set the hyperparameters γ to zero (maximum likelihood estimation). The goodness of the estimation is then measured by the average squared error of the input parameters,

$$E = \frac{1}{m} \sum_{i=1}^{m} \left[(\hat{\mu}_i - \mu)^2 + (\hat{\sigma}_i - \sigma)^2 \right], \tag{25}$$

where $\hat{\mu}_i$ and $\hat{\sigma}_i$ are the estimated input mean and fluctuation amplitude for the ith spike train. The distributions of the functional families that produced the minimum squared error for various sets of input parameters (μ, σ) are displayed in Fig. 2A, where m is set at 1,000. The distributions show that in the biologically plausible region where the coefficient of variation (Cv) of a spike train is around less than 1.5 [28, 30], the gamma and inverse Gaussian distributions worked well compared to the others. Because the ratio of the squared error for the gamma distribution to that for the inverse Gaussian distribution is less than 1.7 (not shown in Fig. 2), the gamma distribution function generally gives the best estimation. Figure 2B displays the ratio of the average estimation error with the gamma distribution to that for the direct method with $m = 100$, showing that the transformation method with the gamma distribution performs well even compared to the direct one. In addition, the computation for the transformation method is very fast (Fig. 2C). Thus, in what follows, we adopt the gamma distribution for fitting the ISI distribution of the OUP.

5.2. **Evaluating the estimation methods with synthetic data.** We compared the direct and transformation methods with respect to their accuracy in estimating the input parameters from the spike trains generated by LIF models with specific time-varying input parameters.

We generated spikes using the standard LIF model (1) and the adaptive LIF model (3) under the time-varying input conditions,

$$\mu(t) = \mu_0 + \delta\mu \sin(\omega t) \tag{26}$$

$$\sigma(t) = \sigma_0 + \delta\sigma \sin(\omega t + \phi), \tag{27}$$

where we specified $\mu_0 = 0.5$ [nA], $\delta\mu = 0.1$ [nA], $\sigma_0 = 0.8$ [nA·ms$^{1/2}$], $\delta\sigma = 0.5$ [nA·ms$^{1/2}$], and $\phi = \pi/2$ for the standard LIF model, and $\mu_0 = 1.0$ [nA], $\delta\mu = 0.7$ [nA], $\sigma_0 = 3$ [nA·ms$^{1/2}$], $\delta\sigma = 2$ [nA·ms$^{1/2}$], and $\phi = \pi/2$ for the adaptive LIF model, with the periods of input fluctuation for both models specified as $T = 2\pi/\omega = 0.5, 1, 1.5, 2, 2.5, 3$ [s]. Figures 3A and 3B display sample estimations by both the direct (red or light gray) and transformation (blue or dark grey) methods for the period $T = 3$ [s].

Comparison of the direct and transformation methods. We evaluated the goodness of each input estimation method in terms of the integrated squared error (ISE) between the intended input parameters and the estimated parameters:

$$\mathrm{ISE} = \frac{1}{10T} \int_0^{10T} dt \left[(\hat{\mu}(t) - \mu(t))^2 + (\hat{\sigma}(t) - \sigma(t))^2 \right]. \tag{28}$$

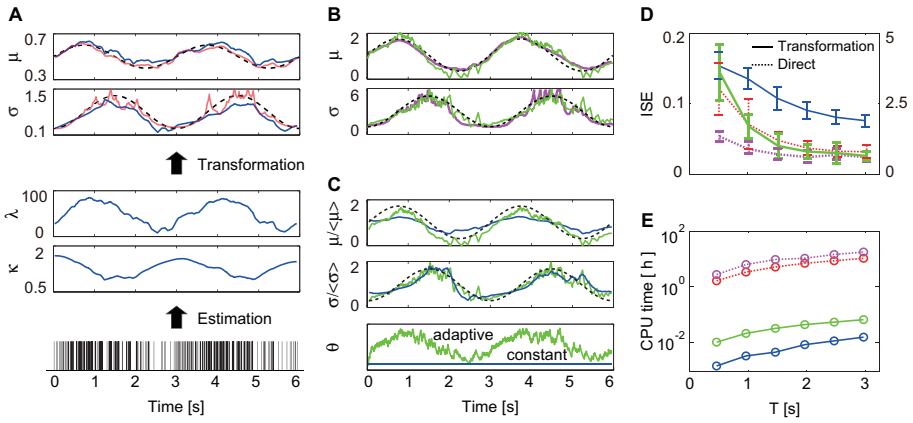

FIGURE 3. Estimation of fluctuating input parameters with synthetic data. (A) The estimated input parameters obtained using the direct (red or light gray) and the transformation (blue or dark grey) method, based on the standard LIF model. In the transformation method, we evaluate the two firing characteristics, rate λ and irregularity κ, from a sample spike train, then we transform the information into most likely input parameters. (B) The estimated input parameters based on the adaptive LIF model, with the direct (green or light gray) and the transformation (magenta or dark grey) method. (C) The estimated input parameters normalized by their own average, obtained using the adaptive (green or light gray) and the standard (blue or dark grey) LIF model. The data was generated with the adaptive LIF model. The bottom panel displays the trajectory of the thresholds in the adaptive and standard LIF models. (D) The ISE between the intended input parameters and estimated parameters against the period of the input modulation T. The scales on the left vertical axis indicate the ISE values for the standard LIF model (blue and red), and those for the adaptive LIF model (green and magenta) are to be read from the right axis. (E) Computational cost of the direct and transformation method for analyzing a $10T$ of spike train, comprising about 300, 600, 800, 1,200, 1,400, and 1,600 ISIs for the periods $T = 0.5, 1, 1.5, 2, 2.5, 3$ [s], respectively.

Figure 3D compares the ISEs of the two methods as plotted against the period of the input modulation, demonstrating that the transformation method can provide accurate estimations compared to the direct method, and with a significantly shorter computation time (Fig. 3E). The difference in ISEs' scales between standard and adaptive LIF models is due to the values of the input parameters to estimate. Because of its computational cost, the direct method is impracticable for analyzing biological data, which typically contain more than several hundred spikes, while the transformation method can analyze thousands of spike trains, each of which contains thousands of spikes.

Comparison of the non-adaptive and adaptive LIFs. Here, we examine what happens when the standard (non-adaptive) LIF models are employed to analyze spike trains derived from adaptive LIFs. To eliminate the dependence of estimated values on the model parameter settings, we used input parameters normalized by their own averages. Figure 3C displays sample input trajectories (black dashed line) and estimated trajectories based on the standard (magenta) and adaptive LIF (green) models, given the same spike train data used for Fig. 3B. Figure 3C shows that when the threshold dynamics are ignored, the dynamic behavior of the input fluctuation can be inferred correctly, but the modulation in the input mean is substantially underestimated. The adaptive threshold produces a negative correlation in successive ISIs, which decreases the modulation in the output firing rate, and as a result, the modulation in the input mean is underestimated. Although the estimation method based on the standard LIF model can also capture the qualitative behavior of inputs, it is essential to include an appropriate modeling of threshold adaptation for the quantitative analysis of input signals.

We also note that our current proposal for fitting the moments works quite efficiently.

6. **Discussion.** We have developed a method for estimating nonstationary input parameters from a single train of neuronal spikes. We have added an adaptive threshold in the LIF generative model and proposed a new principle for fitting the exponential family of distribution functions based on the first two moments. Our transformation method for estimation proved to perform well in place of the direct inference method, which is computationally infeasible for a data set comprising thousands of spikes.

We compared the four representative exponential families based on the goodness of their input estimations, finding that the gamma and inverse Gaussian distributions work better than the normal and log-normal distribution functions in the region of input parameters that generate biologically plausible firing characteristics. This result is consistent with the previous report [9] that neuronal activity can be modeled with a good fit using the generalized inverse Gaussian distribution, which includes the gamma and inverse Gaussian distributions. We also found that the gamma distribution works poorly for highly irregular firing regimes; this may be due to the fact that the maximum likelihood estimator of the shape parameter in the gamma distribution has a large positive bias [4].

Utilizing the fact that the first and second moments of the LIF model with an exponentially decaying threshold can be obtained analytically as expansions in terms of the small threshold modification ϵ_j, we proposed an estimation method that is applicable to the adaptive LIF models. We confirmed in a simulation analysis that the expansion formula works robustly even for $\epsilon_j \sim 2$, where the output firing rate is over 100 Hz. However, it has been reported that the formula sometimes yields negative moments for large values of ϵ_j [15], and therefore, it is worth investigating whether the algorithm can calculate the moments quickly and robustly for even larger values of ϵ_j.

Because the mean drift and uncorrelated fluctuation of input are related to the rates of excitatory and inhibitory input spikes [34, 12, 11], we can investigate the existence of balanced regime of a neuronal network from the behavior of uncorrelated Gaussian input. The covariation between excitatory and inhibitory activities has recently been analyzed in the cerebral cortex by carefully observing temporal

modulation of synaptic conductances [31, 36, 7], although our method does not require anesthesia or significant constraints on the animal when estimating inputs. We can estimate inputs solely from extracellular data.

A notable advantage of our method is its relatively low computational cost. In addition to enable us to analyze large amounts of data, our method enabled us to perform more sophisticated analyses of input signals, combined with computationally expensive techniques such as switching state-space models, hidden Markov models.

Acknowledgments. This study was supported in part by Grants-in-Aid for Scientific Research to SS from the MEXT Japan (20300083, 20020012) and the Global COE Program "The Next Generation of Physics, Spun from Universality and Emergence."

REFERENCES

[1] O. Avila-Akerberg and M. J. Chacron, *Nonrenewal spike train statistics: Causes and functional consequences on neural coding*, Exp. Brain Res., **210** (2011), 353–371.

[2] J. Benda, L. Maler and A. Longtin, *Linear versus nonlinear signal transmission in neuron models with adaptation currents or dynamic thresholds*, J. Neurophysiol., **104** (2010), 2806–2820.

[3] A. Buonocore, A. G. Nobile and L. M. Ricciardi, *A new integral equation for the evaluation of first-passage-time probability densities*, Adv. Appl. Probab., **19** (1987), 784–800.

[4] D. R. Cox and P. A. W. Lewis, "The Statistical Analysis of Series of Events," Methuen & Co., Ltd., London; John Wiley & Sons, Inc., New York, 1966.

[5] S. Ditlevsen and P. Lansky, *Estimation of the input parameters in the Ornstein-Uhlenbeck neuronal model*, Phys. Rev. E, **71** (2005), 011907, 9 pp.

[6] F. Farkhooi, M. F. Strube-Bloss and M. P. Nawrot, *Serial correlation in neural spike trains: Experimental evidence, stochastic modeling, and single neuron variability*, Phys. Rev. E, **79** (2009), 021905.

[7] M. J. Higley and D. Contreras, *Balanced excitation and inhibition determine spike timing during frequency adaptation*, J. Neurosci., **26** (2006), 448–457.

[8] J. Inoue, S. Sato and L. M. Ricciardi, *On the parameter estimation for diffusion models of single neuron's activities*, Biol. Cybern., **73** (1995), 209–221.

[9] S. Iyengar and Q. Liao, *Modeling neural activity using the generalized inverse Gaussian distribution*, Biol. Cybern., **77** (1997), 289–295.

[10] J. Keilson and H. F. Ross, *Passage time distributions for Gaussian Markov (Ornstein-Uhlenbeck) statistical processes*, in "Selected tables in mathematical statistics, Vol. III," Amer. Math. Soc., Providence, RI, (1975), 233–327.

[11] H. Kim and S. Shinomoto, *Estimating nonstationary input signals from a single neuronal spike train*, Phys. Rev. E, **86** (2012), 051903.

[12] P. Lánský and V. Lánská, *Diffusion approximation of the neuronal model with synaptic reversal potentials*, Biol. Cybern., **56** (1987), 19–26.

[13] P. Lánský and S. Ditlevsen, *A review of the methods for signal estimation in stochastic diffusion leaky integrate-and-fire neuronal models*, Biol. Cybern., **99** (2008), 253–262.

[14] N. N. Lebedev, "Special Functions and Their Applications," Revised edition, Dover Publications, Inc., New York, 1972.

[15] B. Lindner and A. Longtin, *Effect of an exponentially decaying threshold on the firing statistics of a stochastic integrate-and-fire neuron*, J. Theor. Biol., **232** (2005), 505–521.

[16] Y.-H. Liu and X.-J. Wang, *Spike-frequency adaptation of a generalized leaky integrate-and-fire model neuron*, J. Comput. Neurosci., **10** (2001), 25–45.

[17] A. Mason and A. Larkman, *Correlations between morphology and electrophysiology of pyramidal neurons in slices of rat visual cortex. II. Electrophysiology*, J. Neurosci., **10** (1990), 1415–1428.

[18] A. Mason, A. Nicoll and K. Stratford, *Synaptic transmission between individual pyramidal neurons of the rat visual cortex in vitro*, J. Neurosci., **11** (1991), 72–84.

[19] D. A. McCormick, B. W. Connors, J. W. Lighthall and D. A. Prince, *Comparative electrophysiology of pyramidal and sparsely spiny stellate neurons of the neocortex*, J. Neurophysiol., **54** (1985), 782–806.
[20] P. Mullowney and S. Iyengar, *Parameter estimation for a leaky integrate-and-fire neuronal model from ISI data*, J. Comput. Neurosci., **24** (2008), 179–194.
[21] M. P. Nawrot, C. Boucsein, V. Rodriguez-Molina, A. Aertsen, S. Grün and S. Rotter, *Serial interval statistics of spontaneous activity in cortical neurons in vivo and in vitro*, Neurocomput., **70** (2007), 1717–1722.
[22] L. Paninski, J. W. Pillow and E. P. Simoncelli, *Maximum likelihood estimation of a stochastic integrate-and-fire neural encoding model*, Neural Comput., **16** (2004), 2533–2561.
[23] L. Paninski, A. Haith and G. Szirtes, *Integral equation methods for computing likelihoods and their derivatives in the stochastic integrate-and-fire model*, J. Comput. Neurosci., **24** (2008), 69–79.
[24] W. H. Press, S. A. Teukolsky, W. T. Vetterling and B. P. Flannery, "Numerical Recipes in C: The Art of Scientific Computing," 2^{nd} edition, Cambridge University Press, Cambridge, 1992.
[25] L. M. Ricciardi and S. Sato, *First-passage-time density and moments of the Ornstein-Uhlenbeck process*, J. Appl. Prob., **25** (1988), 43–57.
[26] Y. Sakai, S. Funahashi and S. Shinomoto, *Temporally correlated inputs to leaky integrate-and-fire models can reproduce spiking statistics of cortical neurons*, Neural Netw., **12** (1999), 1181–1190.
[27] T. Shimokawa and S. Shinomoto, *Estimating instantaneous irregularity of neuronal firing*, Neural Comput., **21** (2009), 1931–1951.
[28] S. Shinomoto, Y. Sakai and S. Funahashi, *The Ornstein-Uhlenbeck process does not reproduce spiking statistics of neurons in prefrontal cortex*, Neural Comput., **11** (1999), 935–951.
[29] A. Smith and E. Brown, *Estimating a state-space model from point process observations*, Neural Comput., **15** (2003), 965–991.
[30] W. R. Softky and C. Koch, *The highly irregular firing of cortical cells is inconsistent with temporal integration of random EPSPs*, J. Neurosci., **13** (1993), 334–350.
[31] Y. Shu, A. Hasenstaub and D. A. McCormick, *Turning on and off recurrent balanced cortical activity*, Nature, **423** (2003), 288–293.
[32] C. F. Stevens and A. M. Zador, *Input synchrony and the irregular firing of cortical neurons*, Nat. Neurosci., **1** (1998), 210–217.
[33] T. W. Troyer and K. D. Miller, *Physiological gain leads to high ISI variability in a simple model of a cortical regular spiking cell*, Neural Comput., **9** (1997), 971–983.
[34] H. C. Tuckwell, "Introduction to Theoretical Neurobiology," Cambridge Studies in Mathematical Biology, No. 8, Cambridge University Press, Cambridge, 1988.
[35] R. D. Vilela and B. Lindner, *Are the input parameters of white noise driven integrate and fire neurons uniquely determined by rate and CV?*, J. Theor. Biol., **257** (2009), 90–99.
[36] M. Wehr and A. M. Zador, *Balanced inhibition underlies tuning and sharpens spike timing in auditory cortex*, Nature, **426** (2003), 442–446.
[37] X. Zhang, G. You, T. Chen and J. Feng, *Maximum likelihood decoding of neuronal inputs from an interspike interval distribution*, Neural Comput., **21** (2009), 3079–3105.

Received December 03, 2012; Accepted June 24, 2013.

E-mail address: kin.hideaki@lab.ntt.co.jp
E-mail address: shinomoto@scphys.kyoto-u.ac.jp